

## Original Article



# Increased Melanoma-Associated Antigen C2 Expression Affords Resistance to Apoptotic Death in Suspension-Cultured Tumor Cells

Doyeon Park <sup>1</sup>, Sora Han <sup>1</sup>, Hyunjeong Joo <sup>1</sup>, Hye In Ka <sup>1</sup>, Sujung Soh <sup>1</sup>, Jiyoung Park <sup>2</sup>, Young Yang <sup>3</sup>

<sup>1</sup>Department of Biological Sciences, Research Center for Cellular Heterogeneity, Research Institute of Women's Health, Sookmyung Women's University, Seoul, Korea

<sup>2</sup>GC LabCell, Yongin, Korea

<sup>3</sup>Department of Biological Sciences, Sookmyung Women's University, Seoul, Korea



Received: Sep 8, 2020

Revised: Dec 5, 2020

Accepted: Dec 18, 2020

### Correspondence to

Young Yang

Department of Biological Sciences,  
Sookmyung Women's University, 99  
Cheongpa-ro 47-gil, Yongsan-gu, Seoul 04312,  
Korea.

E-mail: yyang@sookmyung.ac.kr

© 2021 Korean Breast Cancer Society

This is an Open Access article distributed under the terms of the Creative Commons Attribution Non-Commercial License (<https://creativecommons.org/licenses/by-nc/4.0/>) which permits unrestricted non-commercial use, distribution, and reproduction in any medium, provided the original work is properly cited.

### ORCID iDs

Doyeon Park

<https://orcid.org/0000-0002-5429-461X>

Sora Han

<https://orcid.org/0000-0001-9431-1034>

Hyunjeong Joo

<https://orcid.org/0000-0001-5872-5686>

Hye In Ka

<https://orcid.org/0000-0002-1279-1220>

Sujung Soh

<https://orcid.org/0000-0001-9576-6524>

Jiyoung Park

<https://orcid.org/0000-0002-8206-9508>

Young Yang

<https://orcid.org/0000-0003-4239-0804>

## ABSTRACT

**Purpose:** Melanoma-associated antigen C2 (MAGEC2) is an oncogene associated with various types of cancers. However, the biological function of MAGEC2 in circulating tumor cells remains unclear. In this study, we investigated the role of MAGEC2 using adapted suspension cells (ASCs), which were previously developed to study circulating tumor cells (CTCs).

**Methods:** Differential gene expression in adherent cells (ADs) and ASCs was examined using RNA-seq analysis. MAGEC2 expression was assessed using reverse transcription quantitative polymerase chain reaction (RT-qPCR), immunoblotting, and ChIP-seq analysis. Depletion of MAGEC2 expression was performed using siRNA. MAGEC2-depleted ADs and ASCs were used to investigate changes in the proliferation rate and cell cycle. Then, the protein levels of signal transducer and activator of transcription 3 (STAT3), phosphorylated STAT3, and downstream of STAT3 were measured using control and MAGEC2-depleted ADs and ASCs. In ASCs, the direct effect of active STAT3 inhibition with Stattic, a STAT3 inhibitor, was assessed in terms of proliferation and apoptosis. Finally, an Annexin V/7-AAD assay was performed to determine the percentage of apoptotic cells in the Stattic-treated cells.

**Results:** MAGEC2 was highly expressed in ASCs when compared with ADs. Depletion of MAGEC2 reduced the proliferation rate and viability of ASCs. To elucidate the underlying mechanism, the level of STAT3 was examined owing to its oncogenic properties. Tyrosine-phosphorylated active STAT3 was highly expressed in ASCs and decreased in MAGEC2-depleted ASCs. Furthermore, on treating ASCs with Stattic, an active STAT3 inhibitor, the cells were markedly sensitive to intrinsic pathway-mediated apoptosis.

**Conclusions:** High MAGEC2 expression may play an important role in the survival of ASCs by maintaining the expression of activated STAT3 to prevent apoptotic cell death.

**Keywords:** Breast neoplasms; Neoplasm proteins; Neoplastic cells, circulating; STAT3 transcription factor

**Funding**

Financial support was given by the National Research Foundation of Korea grant funded by the Korean government, MSIT (Ministry of Science and Information and Communication Technology; SRC (Science Research Center) program (Cellular Heterogeneity Research Center: 2016R1A5A1011974 and 2019R111A1A01042695).

**Conflict of Interest**

The authors declare that they have no competing interests.

**Author Contributions**

Conceptualization: Park D, Joo H, Yang Y; Data curation: Joo H, Ka HI, Soh S, Park J; Formal analysis: Park D; Investigation: Park D, Han S; Software: Park D; Supervision: Han S, Yang Y; Validation: Park D, Ka HI; Visualization: Park D; Writing - original draft: Park D; Writing - review & editing: Joo H, Soh S, Yang Y.

**INTRODUCTION**

Metastases and cancer recurrence are widely known to be responsible for a majority of cancer-associated deaths [1]. Circulating tumor cells (CTCs) are derived from primary solid tumor tissues and circulate in the patient's bloodstream, with a fate of death or survival at secondary tumor sites. Thus, it is considered that the survival of CTCs is a critical event for the successful metastatic spread of tumor cells [2]. Nonetheless, the underlying survival mechanism and functional characterization of CTCs remain poorly understood owing to their extreme rarity. To overcome this hurdle and to obtain continuously growing tumor cells in suspension, we previously cultured MDA-MB-468 cells in ultra-low attachment plates [3] for over 6 months, and were named adapted suspension cells (ASCs) [4]. Furthermore, MDA-MB-468 parent cells were named adherent cells (ADs). ASCs exhibit increased expression of silent mating-type information regulation 2 homolog 1 (SIRT1), which contributes to the survival of ASCs by repressing nuclear factor kappa B (NF- $\kappa$ B) and maintaining low levels of reactive oxygen species (ROS). In the present study, we aimed to elucidate additional molecular mechanisms that might affect the survival of ASCs.

Melanoma-associated antigen (MAGE) proteins are classified as cancer-testis antigens (CTAs), which are expressed only in germ cells of the testis and are aberrantly expressed in various human cancers. The MAGE family can be divided into type I and type II MAGEs. Both type I and type II MAGEs share a conserved MAGE homology domain [5]. Type I MAGEs are composed of three subfamilies (MAGE-A, -B, and -C subfamily members) and are all located on the X chromosome [6]. Conversely, type II MAGEs are composed of seven subfamilies (MAGE-D, -E, -F, -G, -H, -L subfamilies, and Necdin), which are expressed in various tissues and are not limited to the X chromosome [7]. Owing to their unusual characteristics, MAGEs are deemed to be ideal targets for cancer therapy [8]. However, the underlying mechanism and biological function of MAGEs remain unclear. MAGEC2, a member of type I MAGEs, is expressed in various cancer types, including breast cancer, prostate cancer, and multiple myeloma. In breast cancer, MAGEC2 expression is associated with poor clinical prognosis and epithelial-mesenchymal transition (EMT) [9,10]. In multiple myeloma, MAGEC2 promotes proliferation independent of p53 [11]. Furthermore, in prostate cancer, MAGEC2 is reportedly a predictor of recurrence and a potential target for cancer therapy [12]. A recent study performed using a melanoma cell line has revealed that MAGEC2 expression induces rounded morphology *in vitro* and promotes metastasis *in vivo* via activation of signal transducer and activator of transcription 3 (STAT3) [13]. This study has revealed that MAGEC2 interacts with tyrosine phosphorylation at the 705 residue of STAT3 and inhibits poly-ubiquitination and proteasomal degradation of STAT3, contributing to the stabilized accumulation of pY-STAT3. Although several studies have documented the oncogenic function of MAEC2 in cancer cells, the biological function of MAGEC2 in CTCs has not been elucidated.

The STAT family is one of the most well-known transcription factor families [14]. Among them, STAT3 has been extensively evaluated as a central mediator of cancer metastasis and a potential target for anticancer drugs [15]. STAT3 upregulates cyclin D1, c-Myc, and Bcl-2 to maintain the survival of tumor cells [16]. Furthermore, STAT3 advances metastasis by upregulating EMT-associated genes such as twist, snail, slug, vimentin, matrix metalloproteinase 2 (MMP-2), and MMP-9. Various cytokines, including interleukin (IL)-6 and IL-10, growth factors, and oncogenic proteins, activate STAT3 [17] through the induction of tyrosine phosphorylation at the 705 residue of STAT3 (Y705) via Janus kinases (JAKs), upon the binding of ligands to their respective receptor [18]. The tyrosine-phosphorylated STAT3

promotes homodimerization and translocates to the nucleus, where it forms a complex with some coactivators and binds to the promoter region of target genes involved in tumorigenesis and cancer progression [15]. In this study, we revealed that overexpression of MAGEC2 in ASCs contributes to the stable accumulation of activated STAT3, thereby contributing to the prevention of apoptotic cell death in ASCs.

## METHODS

### Cell culture

The human breast cancer cell line, MDA-MB-468, was purchased from American Type Culture Collection (ATCC, Manassas, USA). A suspension cell line was established based on a previously published method [3], and cells were cultured for over 150 passages using ultra-low attachment plates (Corning, USA). Both ADs and ASCs were cultured in Roswell Park Memorial Institute (RPMI)-1640 medium (HyClone, Logan, USA), supplemented with 10% heat-inactivated fetal bovine serum (FBS; Equitech-Bio Inc., Kerrville, USA) at 37°C, and incubated under 5% CO<sub>2</sub> humidified atmosphere.

### RNA-seq analysis

RNAs isolated from MDA-MB-468 ADs, ASCs, and secondary solid tumors generated in humanized xenograft mice were used to perform the analysis. In humanized xenograft mice, ADs were transplanted into the mammary fat pad in accordance with a previously described method [4]. Total RNA was prepared using RNAiso Plus (TaKaRa, Shiga, Japan) and cleaned-up using RNA Clean&Concentrator™-25 (Zymo Research, Irvine, USA) following the manufacturer's instructions. Sequencing and analysis of the produced library were conducted by LAS Inc., Seoul, Republic of Korea.

### Reverse transcription-polymerase chain reaction (RT-PCR) analysis

Total RNA was prepared using RNAiso Plus (TaKaRa, Shiga, Japan) following the manufacturer's instructions. Reverse transcription was performed using M-MLV Reverse Transcriptase (Thermo Fisher Scientific, Waltham, USA). SYBR Green (Thermo Fisher Scientific) was used for reverse transcription quantitative polymerase chain reaction (RT-qPCR). The primers used for RT-qPCR amplification were as follows: MAGEA1 forward (5'-AACCTGACCCAGGCTCTGT-3'), MAGEA1 reverse (5'-ATGAAGACCCACAGGCAGAT-3'); MAGEC2 forward (5'-GTGACGAACTGGGTGTGAGG-3'), MAGEC2 reverse (5'-TGGGATGCTGTGCATCTACC-3'); 18srRNA forward (5'-AGCTATCAATCTGTCAATCCTGTC-3'), 18srRNA reverse (5'-CTTAATTGACTCAACACGGGA-3).

### Chromatin immunoprecipitation sequencing/analysis

Briefly, cells were fixed using 1% formaldehyde for 10 minutes, and 0.125 M glycine was used to terminate crosslinking. Nuclei were isolated using Farnham lysis buffer (5 mmol/L PIPES pH 8.0, 85 mmol/L KCl, 0.5% NP-40, and protease inhibitor), followed by fragmentation. Fragmented chromatin (1 mg) was immunoprecipitated with 10 µg H3K27ac, 4 µg H3K4me3 (Millipore, Temecula, USA), and 10 µg RNA Pol II (Abcam, Burlingame, USA). The generated libraries were sequenced using Hi-Seq 2500 (Illumina, San Diego, USA). The human reference genome hg19 was used for aligning the sequenced reads. Integrative Genomics viewer genome browser and HOMER software were used for peak calling and visualization.

### Immunoblotting

Cell lysates were mixed with 5X SDS sample buffer and heated at 99°C for 10 minutes. Whole-cell lysis loaded samples were loaded onto 10% sodium dodecyl sulphate-polyacrylamide gel electrophoresis gels, electrophoresed at 140 V and 400 mA for 1 hour, and then transferred to 0.45 µm nitrocellulose membranes (GE Healthcare, Buckinghamshire, UK) for 2 hours. The membranes were blocked using TBST buffer (20 mmol/L Tris-HCl pH 8.0, 150 mM NaCl pH 7.6, 0.05% Tween 20) with 3% bovine serum albumin (BSA) for 30 minutes. Next, the membranes were incubated with each specific primary antibody at 4°C overnight. Next, the membranes were washed and incubated with horseradish peroxidase-conjugated secondary antibodies for 2 hours at room temperature. The protein bands were visualized using the ECL solution and detected using a LAS3000 luminescent image analyzer (Fuji Film, Tokyo, Japan).

### Cell proliferation assay

In brief, each cell was seeded in triplicate in classic 6-well or ultra-low attachment plates. The cell numbers were manually counted during each time period using hemocytometer cell counting with trypan blue staining.

### Antibodies and reagents

The following antibodies and reagents were purchased: Phospho-Stat Antibody Sampler Kit # 9914T, Death Receptor Antibody Sampler Kit #8356, Caspase-3 #9662S, cleaved caspase-3 #9664, MMP-9 #3852S, and Survivin #2808S (Cell Signaling Technology, Danvers, USA); Anti-MAGEC2 antibody #ab209667 (Abcam, Cambridge, USA); cyclin D1 #sc-718, BID #sc-11423, β-actin #sc-58673 (Santa Cruz Biotechnology, Santa Cruz, USA); PARP #51-6639GR (BD Biosciences, Franklin Lakes, USA); Stattic #S7947 (Sigma-Aldrich, St. Louis, USA).

### siRNA transfection

The cells were transfected using RNAiMax (Invitrogen, Carlsbad, USA) with a siRNA concentration of 20 ng/mL. The siRNAs used for MAGEC2 knockdown were as follows: siMAGEC2-1 (5'-CGAGGAACGUAGUGUUCUU-3') and siMAGEC2-2 (5'-GAUACCGCAGAU GAUGCCAGUGUCA-3').

### Cell cycle analysis

The analysis was performed using PI/RNase staining buffer #550825 (BD Pharmingen; BD Biosciences) according to the manufacturer's protocol. The cells were incubated with 500 nM propidium iodide for 15 min and then analyzed using flow cytometry.

### Immunoprecipitation

In brief, the cells were lysed in lysis buffer (50 mM Tris-HCl pH8.0, 150 mM NaCl, 1 mM ethylenediaminetetraacetic acid, and 1% NP-40, supplemented with a protease and phosphatase cocktail). The lysates were centrifuged for 15 minutes at 4°C at 20,000 × g and the supernatant was used for the experiment. For immunoprecipitation, cell lysates were incubated with 3 µg of the antibody overnight at 4°C and incubated with protein G agarose beads (Amicogen, 2010005) overnight at 4°C. Next, the resulting complexes were washed with lysis buffer 5 times. The final proteins were boiled with 5X SDS and subjected to immunoblotting as described above.

### Immunofluorescence

Experiments were performed as previously described with the following modifications [19]. MAGEC2 gene #RC203064 (OriGene Technologies, Inc., Rockville, USA) was cloned

into the pAdTrack-CMV expression vector, a gift from Bert Vogelstein (Addgene plasmid # 16405; <http://n2t.net/addgene:16405>; RRID:Addgene\_16405). Briefly, cells transfected with pAdTrack-CMV-MAGEC2 and pAdTrack-CMV were fixed using 10% neutral buffered formalin (Sigma-Aldrich) and blocked in phosphate-buffered saline (PBS) with 0.1% BSA at 23°C for 30 min. Then, the fixed cells were immunostained with 7-AAD #51-68981E (BD Pharmingen; BD Biosciences) and permeabilized with 0.1% Triton X-100 (Sigma-Aldrich), followed by immunostaining with active caspase 3 #550821 (BD Pharmingen; BD Biosciences). DNA was stained with Fluoroshield™ with DAPI (Sigma-Aldrich). Confocal still images were obtained with a Zeiss confocal microscope (Carl Zeiss Microscopy GmbH, Jena, Germany).

### Apoptosis detection by Annexin V/7-AAD assay

In brief, cells were plated in a 6-well plate at a density of  $5 \times 10^5$  cells/well on the day before treatment. The control group was treated with 1000X dimethyl sulfoxide (DMSO), while the experimental group was treated with a final concentration of 2  $\mu$ M Stattic. The apoptosis assay was performed 48 hours after Stattic treatment. The assay was performed using Annexin V, Annexin V-FITC /PI #556570, and 7-AAD #51-68981E (BD Pharmingen; BD Biosciences) according to the manufacturer's protocol.

### Statistical analysis

Multiple comparisons were analyzed using a one-way factorial analysis of variance. Individual group mean differences in the main effect were determined using Student's t-test. The  $p < 0.05$  was considered as the threshold.

## RESULTS

### ASCs express high levels of the cancer-testis antigen MAGEC2

Previously, we reported that high SIRT1 expression is associated with the downregulation of ROS in ASCs, a key event for the survival of ASCs [4]. To systemically identify other signaling molecules responsible for the survival of ASCs, differential gene expression between ADs and ASCs was examined using RNA-seq analysis. Accordingly, 1,352 genes were found to be differentially expressed, presenting more than a 2-fold change. Among the differentially expressed genes, several MAGE genes, which are members of CTA genes, were observed (Table 1). Although the expression of CTA genes is limited in reproductive organs, some genes are expressed in tumor tissues. Thus, we focused on elucidating the role of MAGE in ASCs. First, the differences in MAGEA1 and MAGEC2 expression between ADs and ASCs were assessed. Consistent with the results of RNA-seq analysis, ASCs showed a significant increase in MAGEA1 and MAGEC2 expression (Figure 1A), with protein levels increased along with increased mRNA levels (Figure 1B), suggesting that MAGE is increased to play a role in ASCs. In this study, we focused on MAGEC2, as it is highly increased in ASCs. To examine whether promoter regional activation underlies the increased expression, ChIP-seq analysis was performed using antibodies against the promoter opening markers H3K4me3 and H3K27Ac. Although the promoter region of ADs was closed, the promoter region of MAGEC2 was highly occupied by RNA polymerase II, with an opening by modification of H3K4me3 and H3K27Ac (Figure 1C).

### Deficiency of MAGEC2 induces apoptosis in ASCs

To elucidate the role of enhanced MAGEC2 expression, MAGEC2 was reduced by siRNA treatment. Both the designed siMAGEC2 efficiently reduced MAGEC2 expression (Figure 2A).

The Role of MAGEC2 in Suspension-Cultured Tumor Cells

**Table 1.** List of significantly upregulated genes in ASCs compared with ADs

Gene	Description	log <sub>2</sub> FC	p-value
SERPINB10	Serpin peptidase inhibitor, clade B (ovalbumin), member 10	13.7	0.187
UGT1A10	UDP glucuronosyltransferase 1 family, polypeptide A10	10.7	0.423
DCAF4L2	DDB1 and CUL4 associated factor 4-like 2	9.63	0.003
SOHLH2	Spermatogenesis and oogenesis specific basic helix-loop-helix 2	9.22	<i>p</i> < 0.001
MAGEC2	Melanoma antigen family C, 2	8.91	<i>p</i> < 0.001
GULP1	GULP, engulfment adaptor PTB domain containing 1	8.5	0.012
EPHB1	EPH receptor B1	8.18	<i>p</i> < 0.001
GPRIN3	GPRIN family member 3	8.01	0.001
ERMN	Ermin, ERM-like protein	7.73	0.012
SOD3	Superoxide dismutase 3, extracellular	7.34	0.334
MAGEA1	Melanoma antigen family A, 1	4.96	<i>p</i> < 0.001

Gene expression was compared between ADs and ASCs by RNA-seq analysis. Listed genes are highly upregulated in ASCs, as described. FC, fold change; ASC, adapted suspension cell; AD, adherent cell.

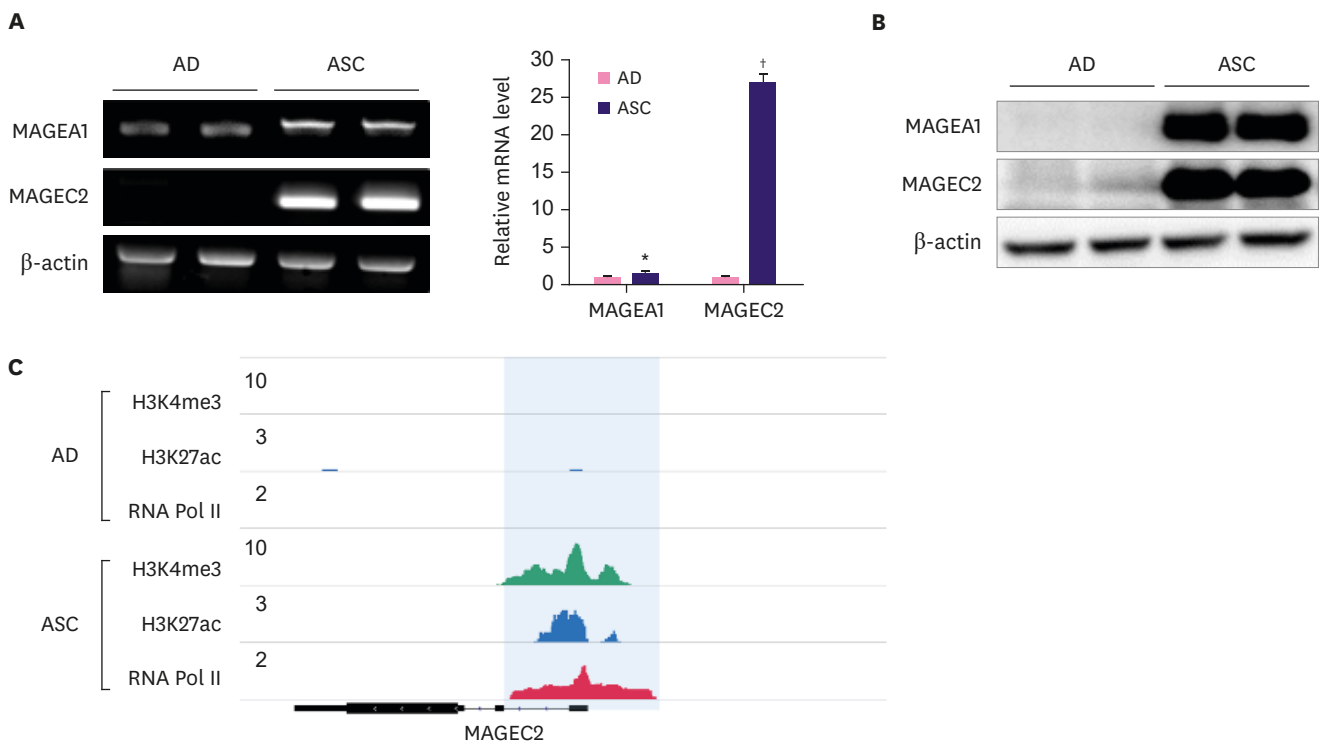


**Figure 1.** MAGEC2 expression in ADs and ASCs.

(A) Expression levels of type I MAGEs in ADs and ASCs were determined by qPCR and RT-PCR. β-actin and 18S rRNA were used for data normalization. (B) Cells were plated in a 6-well plate at a density of  $5 \times 10^5$  per well. Protein levels of MAGEA1 and MAGEC2 in ADs and ASCs were analyzed by immunoblot assay. (C) Visualization of H3K4me3, H3K27ac, and RNA Pol II ChIP-seq near MAGEC2 gene.

MAGE, melanoma-associated antigen; ASC, adapted suspension cell; AD, adherent cell; qPCR, quantitative polymerase chain reaction; RT-PCR, reverse transcription-polymerase chain reaction.

\**p* < 0.01, †*p* < 0.001, Student's t-test.

On measuring the cell number after siMAGEC2 transfection, ASCs showed a 50% decrease in cell number, with ADs also demonstrating a decrease in cell number. However, the ratio of decrease in ASCs was higher than that in ADs (**Figure 2B**). It could be postulated that the increase in MAGEC2 is more highly associated with the proliferation rate of ASCs than that of ADs. To investigate whether the decrease in the proliferation rate of siMAGEC2-treated ASCs was due to changes in the cell cycle, siMAGEC2-treated ASCs were stained with propidium iodide and then analyzed to examine the distribution of each phase of the cell cycle using flow cytometry. Interestingly, ASCs showed an abnormally high level of cell population with

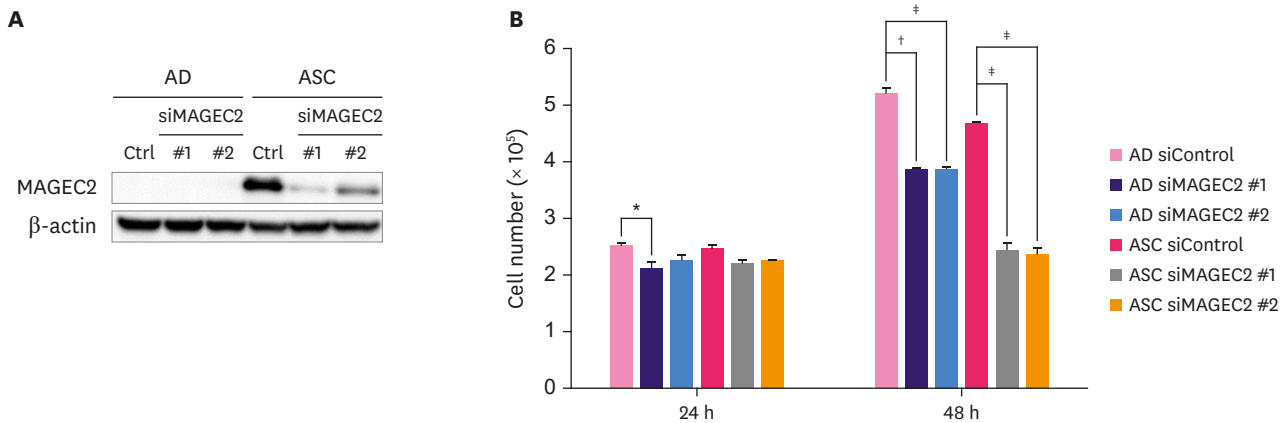


**Figure 2.** MAGEC2 inhibition suppresses ASC proliferation.

(A) Both ADs and ASCs were transfected with siControl or siMAGEC2 at a concentration of 20 ng/mL for 48 hours. The efficiency was evaluated by immunoblot assay. (B) Cells were plated in a 6-well plate at a density of  $2 \times 10^5$  per well. Cell numbers were counted at 24 and 48 hours post-treatment with siRNAs (20 ng/mL). Cell counting was performed in triplicate. Bars represent the mean  $\pm$  standard deviation. One-way ANOVA and Student's t-test were performed to assess the statistical significance ( $p = 0.004$  at the time point of 24 hours, while  $p < 0.001$  at 48 hours, one-way ANOVA).

MAGEC2, melanoma-associated antigen C2; ASC, adapted suspension cell; AD, adherent cell; ANOVA, analysis of variance.

\* $p < 0.05$ , † $p < 0.01$ , ‡ $p < 0.001$ , Student's t-test.

polyploidy, with cells demonstrating an increased DNA content of more than 4N (**Figure 3A**), and the ratio of the subG1 phase, which represents the apoptosis-derived fractional DNA content, markedly increased in MAGEC2-depleted ASCs (**Figure 3B**), indicating that reduction of MAGEC2 expression results in apoptosis in ASCs. As reported in previous studies [20], it appears that polyploid cells underwent apoptosis in the absence of MAGEC2 expression, consequently increasing the subG1 phase. Collectively, these data revealed that the suspension culture could induce polyploidization, with reduced MAGEC2 expression resulting in the induction of apoptosis.

### MAGEC2 is involved in the activation of STAT3 in ASCs

To further investigate the molecular mechanisms via which MAGEC2 plays a role in preventing apoptosis of ASCs, the binding partners of MAGEC2 were searched in the PubMed database. STAT3 [13] is generally known as an essential mediator of cancer metastasis and invasion [21]. Therefore, the basal protein levels of total STAT3 and tyrosine 705-phosphorylated STAT3 (pY-STAT3), an active form of STAT3, were examined in ADs and ASCs. No difference was observed in the total amount of STAT3, whereas pY-STAT3 expression was significantly increased in ASCs (**Figure 4A**). Next, as previous studies have reported that MAGEC2 contributes to sustaining high levels of pY-STAT3 by inhibiting ubiquitination and proteasomal degradation [13], we investigated whether increased pY-STAT3 in ASCs is also related to ubiquitination. The ubiquitinated status of pY-STAT3 was investigated in both ADs and ASCs, pre-treated with 20  $\mu$ M MG132 for 10 hours by immunoprecipitation. In the present study, the polyubiquitination of pY-STAT3 was significantly lower in ASCs (**Figure 4B**), suggesting that, as in previous studies, MAGEC2 is involved in regulating the ubiquitination of pY-STAT3 in ASCs. To examine whether MAGEC2 affects the phosphorylation of STAT3, the protein levels of STAT3, pY-STAT3, and serine 727-phosphorylated STAT3 (pS-STAT3) were determined in ASCs transfected with siMAGEC2. MAGEC2 downregulation resulted in a comparable reduction in pY-STAT3 expression levels (**Figure 4C**), but not in pS-STAT3, in line with the previous study revealing that MAGEC2 accumulates active STAT3. Next, the protein levels of the STAT3 downstream target genes, cyclin D1, MMP-9, and survivin, were measured in MAGEC2-depleted ADs and

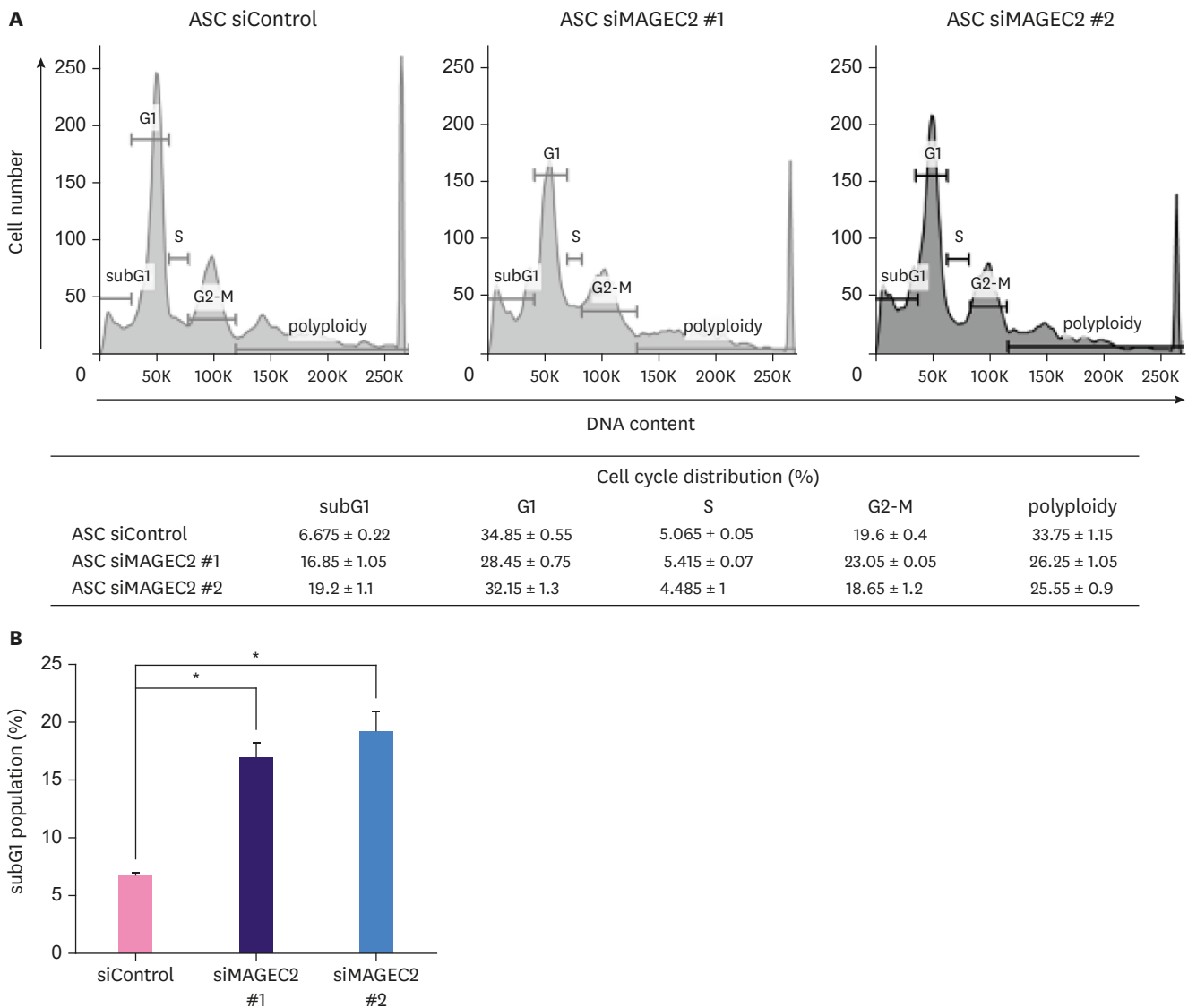


**Figure 3.** Downregulation of MAGEC2 promotes apoptosis of ASCs.

(A) ASCs were transfected with siControl or siMAGEC2 and harvested after 48 h. Harvested cells were stained with propidium iodide and subjected to flow cytometric analysis. The analysis was performed in duplicate and representative data are shown in the figure. (B) The graph indicates the percentage distribution of the subG1 population in ASCs. Bars represent the mean ± standard deviation ( $p < 0.001$ , one-way ANOVA).

MAGEC2, melanoma-associated antigen C2; ASC, adapted suspension cell; ANOVA, analysis of variance.

\* $p < 0.01$ , Student's t-test.

ASCs. Depletion of MAGEC2 in both ADs and ASCs reduced the expression levels of target genes; however, no significant difference was observed in patterns between ADs and ASCs (Figure 4D). The reason underlying the similar expression levels of STAT3 target genes in ADs, in which MAGEC2 expression was not observed, was intriguing. To resolve this discrepancy, cell lysates of only ADs were analyzed through over-exposure of immunoblots to determine whether MAGEC2 expression was detected. Accordingly, it was observed that ADs express low amounts of MAGEC2, and treatment with siMAGEC2 effectively reduced the level of MAGEC2 (Figure 4E). These findings suggest that MAGEC2 may be involved in the STAT3 signaling pathway in both ADs and ASCs, regardless of the underlying expression level of MAGEC2.



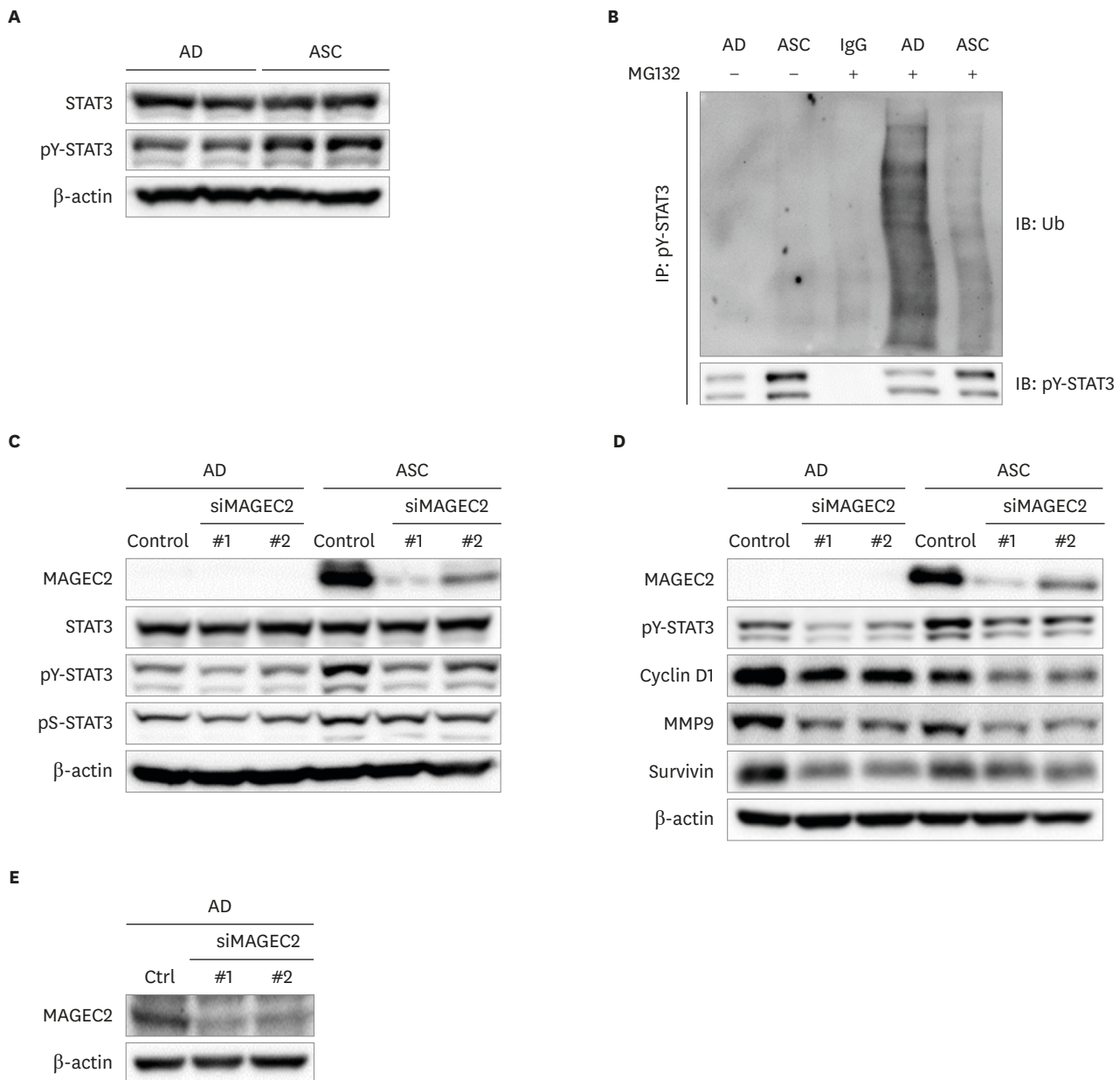


**Figure 4.** MAGEC2 contributes to STAT3 hyperactivation in ASCs.

(A) Levels of total STAT3 and pY-STAT3 in the basal ADs and ASCs were evaluated by immunoblot assay. (B) Cells were lysed in the presence or absence of MG132 20  $\mu$ M for 10 hours and immunoprecipitated with pY-STAT3. Endogenous levels of poly-ubiquitinated pY-STAT3 and pY-STAT3 were measured by immunoblotting. (C) Cells were transfected with siControl or siMAGEC2 for 48 hours and levels of STAT3, pY-STAT3, and pS-STAT3 were evaluated. (D) Protein levels of STAT3 downstream target genes, cyclin D1, MMP9, and survivin, were examined by immunoblot assays in cells treated with siControl and siMAGEC2. (E) Depletion of siMAGEC2 efficiency in ADs was evaluated by over-exposure immunoblotting.

MAGEC2, melanoma-associated antigen C2; ASC, adapted suspension cell; AD, adherent cell; STAT3, signal transducer and activator of transcription 3; MMP-9; matrix metalloproteinase 9.

### ASCs are highly sensitive to apoptosis by inhibiting active STAT3

As no difference was observed in the expression of the target protein of STAT3 between ADs and ASCs, active STAT3 was suppressed by treatment with an active STAT3 inhibitor, Stattic, to investigate the role of active STAT3 in ASCs. On treating ADs and ASCs with 2  $\mu$ M Stattic, a significant difference in cell number was detected. On day 1 following treatment, the proliferation of Stattic-treated ASCs decreased by over 50% when compared

with the control ASCs, while Stattic-treated ADs decreased by approximately 25% when compared with that of control ADs (**Figure 5A**). On day 2, the viability of Stattic-treated ASCs decreased dramatically, indicating that ASCs are more sensitive to the inhibition of STAT3 activation when compared with ADs. As the inhibition of STAT3 activation results in a dramatic decrease in cell number, we next determined whether treatment with Stattic induces apoptosis. Stattic-treated-ASCs presented highly increased protein levels of cleaved caspase-3, caspase-7, and poly(ADP-ribose) polymerase (PARP) when compared with ADs (**Figure 5B**). Furthermore, the level of apoptosis inhibitor protein XIAP (X-linked inhibitor of apoptosis protein) was significantly reduced in Stattic-treated ASCs, indicating that ASCs are more susceptible to apoptosis induction when compared with ADs following inhibition of active STAT3. Next, the levels of anti-apoptotic proteins were assessed in ASCs treated with Stattic (**Figure 5C**). It was observed that the Bcl-2 family, which is part of the intrinsic apoptotic pathway, including Bcl-2, Bcl-XL, and Mcl-1, is decreased in Stattic-treated ASCs but not in Stattic-treated ADs. Then, the levels of proteins related to extrinsic apoptotic pathway signals were examined, and no significant differences were observed. Although FAS is increased in ASCs, treatment with Stattic did not affect FAS levels. Finally, early and late apoptosis were assessed after Stattic treatment using the Annexin V/7-AAD staining assay. Flow cytometry analysis revealed that the ratio of both early and late apoptotic cells significantly increased in 2  $\mu$ M Stattic-treated ASCs. The percentage of apoptotic cells increased from 2.2% to 21.2%, with only a slight increase in apoptotic cells in Stattic-treated ADs (**Figure 5D**). These results indicate that active STAT3 contributes to resistance to apoptotic signals in ASCs.

## DISCUSSION

Metastasis and cancer recurrence remain major causes of cancer-associated deaths. During EMT and mesenchymal–epithelial transition (MET), which are prerequisite processes of metastasis, CTCs originating from primary tumor sites are present in the patient's blood. Thus, a clear characterization of CTCs is necessary to prevent patient death. Several studies have revealed that CTCs generally demonstrate a short survival time in the patient's blood [22]. However, CTCs are widely known to be heterogeneous [23], indicating that not all subsets present the same phenotype. Some CTC subsets exhibit stemness properties, which are termed circulating cancer stem cells (CSCs). CSCs possess high invasiveness and metastatic potential [24]. In the present study, we demonstrated that ASCs have characteristics of both CSCs and CTCs. Furthermore, some subsets of ASCs may be CSCs. Thus, we believe that ASCs are an excellent culture model for investigating CTCs containing CSCs.

CTAs are suggested as unique potential biomarkers of CSCs as they are more frequently expressed in CSCs when compared with those of differentiated cells [25,26]. We revealed that ASCs show high expression levels of CTAs, including the MAGE family. The MAGE family member presenting the highest expression level was MAGEC2 in ASCs derived from MDA-MB-468 cells. It was considered that MAGEC2 overexpression may contribute to the stemness features of ASCs and extend survival in the suspension culture condition. To generalize this concept, we obtained ASCs from several breast cancer cell lines. However, not all ASCs showed high expression levels of MAGEC2 (**Supplementary Figure 1**). In further studies, ASCs derived from luminal A and B, basal-like, and triple-negative breast cancers should be used to comprehensively define the role of MAGE family expression.

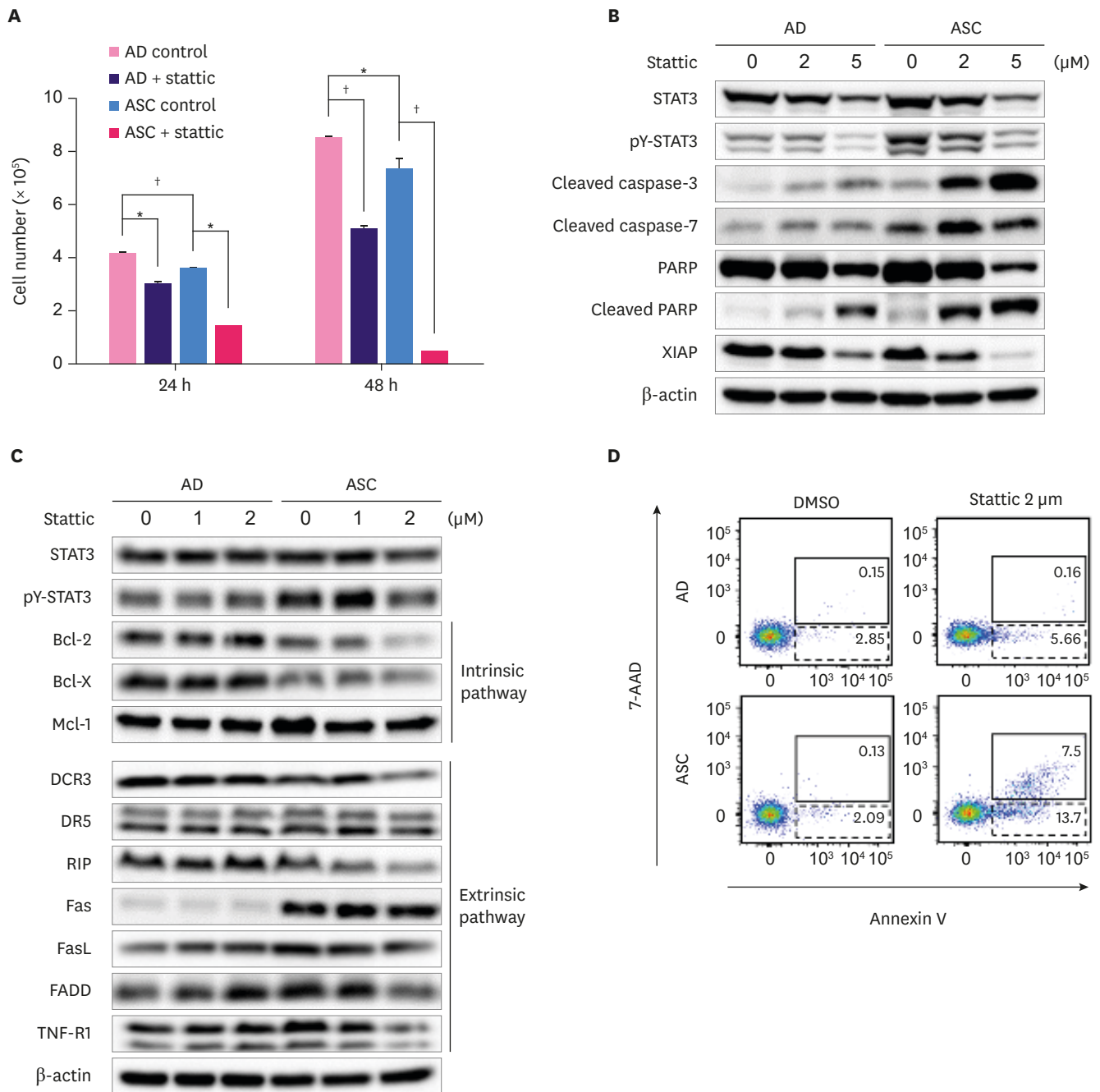


**Figure 5.** Inhibition of active STAT3 results in the induction of apoptotic cell death in ASCs.

(A) Cells were plated in a 6-well plate at a density of  $2 \times 10^5$  per well and were then treated with  $2 \mu\text{M}$  Stattic or DMSO. The number of cells was counted at 24 and 48 hours after treatment. The cell proliferation assay was performed in triplicate ( $p < 0.001$  at the time point of 24 hours, while  $p < 0.001$  at 48 hours, one-way ANOVA). (B) Levels of cleaved caspase-3 and -7, PARP, cleaved PARP, and XIAP were determined in cells treated with 2 and  $5 \mu\text{M}$  of Stattic by immunoblot assay. (C) Levels of Bcl-2 family members, Bcl-2, Bcl-X, and Mcl-1, in ADs and ASCs treated at indicated Stattic concentrations were examined by immunoblot assay. These proteins are labeled as the intrinsic pathway on the right. Levels of death receptor signaling related proteins in Stattic-treated cells were investigated by immunoblot assay. These proteins are labeled as the extrinsic pathway on the right. (D) ADs and ASCs were plated in a 6-well plate at a density of  $5 \times 10^5$  per well and were treated with  $2 \mu\text{M}$  Stattic for 48 hours. Harvested cells were stained with Annexin V/7-AAD for 15 minutes and subjected to flow cytometric analysis. The frame with dashed and solid lines refer to early apoptotic cells and late apoptotic cells, respectively. STAT3, signal transducer and activator of transcription 3; ASC, adapted suspension cell; AD, adherent cell; PARP, poly(ADP-ribose) polymerase.

\* $p < 0.01$ , † $p < 0.001$ , Student's t-test.

Accumulating evidence suggests that STAT3 plays a key role in the survival of cancer cells. Recently, a new biological function of STAT3 has been uncovered in breast CSCs. STAT3 activation is required for the maintenance, promotion, regulation, and expansion of CSCs [27,28]. Moreover, activation of STAT3 protects CTCs by secretion of immunosuppressive factors, thereby protecting CTCs from immune surveillance. Therefore, it is conceivable that STAT3 activation contributes to the survival of CTCs. In this study, the expression level of active STAT3 significantly increased in ASCs when compared to ADs. Inhibition of active STAT3 dramatically induced apoptotic cell death in ASCs. This implies that a higher level of active STAT3 should be maintained in ASCs than in ADs. Furthermore, MAGEC2 overexpression in ADs demonstrated no significant changes in either STAT3 activation or apoptosis (**Supplementary Figure 2**). This is probably because MAGEC2 does not play an essential role in cell survival under normal conditions of ADs, while an increase in MAGEC2 and active STAT3 is important for the survival of cancer cells in suspension. Thus, the life and death of ADs can be deemed MAGEC2-independent, while MAGEC2-dependent in ASCs. However, in the present study, depletion of MAGEC2 in ADs also resulted in reduced protein expression levels of STAT3 downstream target genes, cyclin D1, MMP-9, and survivin. As MAGEC2 and active STAT3 are significantly increased in ASCs and are important for the survival of ASCs, we postulate that there may be other target genes of STAT3 that may exhibit MAGEC2-associated STAT3 function only in ASCs.

A previous study has revealed that MAGEC2 interacts with pY-STAT3 in the nucleus of cancer cells and inhibits polyubiquitination and proteasome degradation, thereby supporting the maintenance of highly activated STAT3, and MAGEC2 expression is associated with increased metastasis [13]. In the present study, MAGEC2 inhibition blocked the activation of STAT3, as well as the expression of STAT3 downstream targets. This result is consistent with a previous study performed using melanoma cell lines. Furthermore, a noticeable difference was observed between ADs and ASCs when treated with an active STAT3 inhibitor. Compared with ADs, apoptosis of ASCs was more highly induced by a low dose of the inhibitor. Therefore, the increased MAGEC2 expression in ASCs is essential to maintain increased STAT3 activation for survival.

ASCs possess an abnormally high proportion of polyploid populations. Previous studies have shown that polyploid CTCs are frequently detected in diverse types of cancers and that the number of patients with polyploid CTCs is highly distributed in stages III and IV than stages I and II [29]. MAGEC2-depleted ASCs resulted in a reduced polyploidy ratio when compared with control ASCs (**Figure 3A**). It is known that polyploid cells undergo apoptosis at a higher rate [20]. In a previous study, we observed that ASCs undergo rapid apoptosis and proliferation. Therefore, we believe that the high proportion of polyploid cells in ASCs is associated with rapid apoptosis. Furthermore, the inhibition of apoptosis accumulates in the polyploid population, and apoptosis induced by the intrinsic pathway contributes to the elimination of polyploid cells [30]. In this study, we demonstrated that high MAGEC2 expression prevents apoptosis of ASCs, which may underlie the accumulation of polyploid populations, and depletion of MAGEC2 resulted in the elimination of polyploid cells, consistent with previous studies.

For clinical significance, The Cancer Genome Atlas data were evaluated to systematically determine whether MAGEC2 expression is related to the overall survival of patients with breast cancer. Based on the mRNA expression levels of MAGEC2, MAGEC2-high, and MAGEC2-low patient groups were set at the top and bottom 15%, respectively. The MAGEC2-high patient group revealed a shorter duration of survival when compared with the MAGEC2-

low patient group (**Supplementary Figure 3**). Moreover, MDA-MB-468 parent cells were injected into immunodeficient mice to generate a xenograft model for human mammary tumor metastasis. Consequently, a secondary solid tumor was formed and used for RNA-seq analysis, revealing that MAGEC2 expression was significantly increased in secondary solid tumors when compared with that in ADs (**Supplementary Table 1**). Thus, in terms of clinical significance, the increased expression of MAGEC2 will be positively involved in tumor metastasis. Nevertheless, there is a lack of information regarding medications or types of chemotherapy for each patient and chemoresistance in patients, warranting further study. These findings highlight the importance of investigating MAGEC2-associated pathways and suggest that MAGEC2 is a potential target for breast cancer treatment. In conclusion, ASCs exhibit a short survival time, but owing to the presence of CSCs in ASCs, ASCs can continue to proliferate. In this study, we demonstrated that MAGEC2 and active STAT3 are highly expressed in ASCs. High expression of MAGEC2 contributes to the maintenance of hyperactivated STAT3 in ASCs, which is an essential survival strategy in the growth environment of ASCs. Therefore, we propose that MAGEC2 is a potential therapeutic target for treating breast cancer metastasis.

## SUPPLEMENTARY MATERIALS

### Supplementary Table 1

MAGEC2 expression in secondary solid tumor

[Click here to view](#)

### Supplementary Figure 1

MAGEC2 expression levels in ASCs derived from other breast cancer cell lines.

[Click here to view](#)

### Supplementary Figure 2

Overexpression of MAGEC2 in ADs.

[Click here to view](#)

### Supplementary Figure 3

A plot of OS analysis in patients with invasive breast carcinoma by Kaplan-Meier analysis.

[Click here to view](#)

## REFERENCES

1. Nguyen DX, Bos PD, Massagué J. Metastasis: from dissemination to organ-specific colonization. *Nat Rev Cancer* 2009;9:274-84.  
[PUBMED](#) | [CROSSREF](#)
2. Pantel K, Brakenhoff RH, Brandt B. Detection, clinical relevance and specific biological properties of disseminating tumour cells. *Nat Rev Cancer* 2008;8:329-40.  
[PUBMED](#) | [CROSSREF](#)

3. Park JY, Jeong AL, Joo HJ, Han S, Kim SH, Kim HY, et al. Development of suspension cell culture model to mimic circulating tumor cells. *Oncotarget* 2017;9:622-40.  
[PUBMED](#) | [CROSSREF](#)
4. Park JY, Han S, Ka HI, Joo HJ, Soh SJ, Yoo KH, et al. Silent mating-type information regulation 2 homolog 1 overexpression is an important strategy for the survival of adapted suspension tumor cells. *Cancer Sci* 2019;110:2773-82.  
[PUBMED](#) | [CROSSREF](#)
5. Doyle JM, Gao J, Wang J, Yang M, Potts PR. MAGE-RING protein complexes comprise a family of E3 ubiquitin ligases. *Mol Cell* 2010;39:963-74.  
[PUBMED](#) | [CROSSREF](#)
6. Simpson AJ, Caballero OL, Jungbluth A, Chen YT, Old LJ. Cancer/testis antigens, gametogenesis and cancer. *Nat Rev Cancer* 2005;5:615-25.  
[PUBMED](#) | [CROSSREF](#)
7. Barker PA, Salehi A. The MAGE proteins: emerging roles in cell cycle progression, apoptosis, and neurogenetic disease. *J Neurosci Res* 2002;67:705-12.  
[PUBMED](#) | [CROSSREF](#)
8. Cameron BJ, Gerry AB, Dukes J, Harper JV, Kannan V, Bianchi FC, et al. Identification of a Titin-derived HLA-A1-presented peptide as a cross-reactive target for engineered MAGE A3-directed T cells. *Sci Transl Med* 2013;5:197ra103.  
[PUBMED](#) | [CROSSREF](#)
9. Zhao Q, Xu WT, Shalieer T. Pilot study on MAGE-C2 as a potential biomarker for triple-negative breast cancer. *Dis Markers* 2016;2016:2325987.  
[PUBMED](#) | [CROSSREF](#)
10. Yang F, Zhou X, Miao X, Zhang T, Hang X, Tie R, et al. MAGEC2, an epithelial-mesenchymal transition inducer, is associated with breast cancer metastasis. *Breast Cancer Res Treat* 2014;145:23-32.  
[PUBMED](#) | [CROSSREF](#)
11. Lajmi N, Luetkens T, Yousef S, Templin J, Cao Y, Hildebrandt Y, et al. Cancer-testis antigen MAGEC2 promotes proliferation and resistance to apoptosis in Multiple Myeloma. *Br J Haematol* 2015;171:752-62.  
[PUBMED](#) | [CROSSREF](#)
12. von Boehmer L, Keller L, Mortezaei A, Provenzano M, Sais G, Hermanns T, et al. MAGE-C2/CT10 protein expression is an independent predictor of recurrence in prostate cancer. *PLoS One* 2011;6:e21366.  
[PUBMED](#) | [CROSSREF](#)
13. Song X, Hao J, Wang J, Guo C, Wang Y, He Q, et al. The cancer/testis antigen MAGEC2 promotes amoeboid invasion of tumor cells by enhancing STAT3 signaling. *Oncogene* 2017;36:1476-86.  
[PUBMED](#) | [CROSSREF](#)
14. Levy DE, Lee CK. What does Stat3 do? *J Clin Invest* 2002;109:1143-8.  
[PUBMED](#) | [CROSSREF](#)
15. Devarajan E, Huang S. STAT3 as a central regulator of tumor metastases. *Curr Mol Med* 2009;9:626-33.  
[PUBMED](#) | [CROSSREF](#)
16. Chun J, Song K, Kim YS. Sesquiterpene lactones-enriched fraction of *Inula helenium* L. induces apoptosis through inhibition of signal transducers and activators of transcription 3 signaling pathway in MDA-MB-231 breast cancer cells. *Phytother Res* 2018;32:2501-9.  
[PUBMED](#) | [CROSSREF](#)
17. Wegenka UM, Buschmann J, Lütticken C, Heinrich PC, Horn F. Acute-phase response factor, a nuclear factor binding to acute-phase response elements, is rapidly activated by interleukin-6 at the posttranslational level. *Mol Cell Biol* 1993;13:276-88.  
[PUBMED](#) | [CROSSREF](#)
18. Ma JH, Qin L, Li X. Role of STAT3 signaling pathway in breast cancer. *Cell Commun Signal* 2020;18:33.  
[PUBMED](#) | [CROSSREF](#)
19. Han S, Jeong AL, Lee S, Park JS, Buyanravjikh S, Kang W, et al. C1q/TNF- $\alpha$ -related protein 1 (CTRPI) maintains blood pressure under dehydration conditions. *Circ Res* 2018;123:e5-19.  
[PUBMED](#) | [CROSSREF](#)
20. Hsieh TC, Traganos F, Darzynkiewicz Z, Wu JM. The 2,6-disubstituted purine reversine induces growth arrest and polyploidy in human cancer cells. *Int J Oncol* 2007;31:1293-300.  
[PUBMED](#) | [CROSSREF](#)
21. Yu H, Jove R. The STATs of cancer--new molecular targets come of age. *Nat Rev Cancer* 2004;4:97-105.  
[PUBMED](#) | [CROSSREF](#)
22. Agnoletto C, Corrà F, Minotti L, Baldassari F, Crudele F, Cook WJ, et al. Heterogeneity in circulating tumor cells: the relevance of the stem-cell subset. *Cancers (Basel)* 2019;11:483.  
[PUBMED](#) | [CROSSREF](#)

23. Bednarz-Knoll N, Alix-Panabières C, Pantel K. Clinical relevance and biology of circulating tumor cells. *Breast Cancer Res* 2011;13:228.  
[PUBMED](#) | [CROSSREF](#)
24. Meng S, Tripathy D, Frenkel EP, Shete S, Naftalis EZ, Huth JF, et al. Circulating tumor cells in patients with breast cancer dormancy. *Clin Cancer Res* 2004;10:8152-62.  
[PUBMED](#) | [CROSSREF](#)
25. Gordeeva O. Cancer-testis antigens: unique cancer stem cell biomarkers and targets for cancer therapy. *Semin Cancer Biol* 2018;53:75-89.  
[PUBMED](#) | [CROSSREF](#)
26. Yawata T, Nakai E, Park KC, Chihara T, Kumazawa A, Toyonaga S, et al. Enhanced expression of cancer testis antigen genes in glioma stem cells. *Mol Carcinog* 2010;49:532-44.  
[PUBMED](#) | [CROSSREF](#)
27. Carneiro Leão G, Magalhães Filho M, Galvão LP, Machado RC, Padovan IP, Jucá NT, et al. Occurrence of *Campylobacter pylori* in patients with gastritis and peptic ulcer. *Arq Gastroenterol* 1988;25:23-8.  
[PUBMED](#)
28. Yu H, Lee H, Herrmann A, Buettner R, Jove R. Revisiting STAT3 signalling in cancer: new and unexpected biological functions. *Nat Rev Cancer* 2014;14:736-46.  
[PUBMED](#) | [CROSSREF](#)
29. Ye Z, Ding Y, Chen Z, Li Z, Ma S, Xu Z, et al. Detecting and phenotyping of aneuploid circulating tumor cells in patients with various malignancies. *Cancer Biol Ther* 2019;20:546-51.  
[PUBMED](#) | [CROSSREF](#)
30. Castedo M, Coquelle A, Vivet S, Vitale I, Kauffmann A, Dessen P, et al. Apoptosis regulation in tetraploid cancer cells. *EMBO J* 2006;25:2584-95.  
[PUBMED](#) | [CROSSREF](#)